



| | |
|-------------------------|--|
| Title | In situ X-ray photoelectron spectroscopy using a conventional Al-K alpha source and an environmental cell for liquid samples and solid-liquid interfaces |
| Author(s) | Endo, Raimu; Watanabe, Daisuke; Shimomura, Masaru; Masuda, Takuya |
| Citation | Applied physics letters, 114(17), 173702 https://doi.org/10.1063/1.5093351 |
| Issue Date | 2019-04-29 |
| Doc URL | http://hdl.handle.net/2115/77739 |
| Rights | This article may be downloaded for personal use only. Any other use requires prior permission of the author and AIP Publishing. This article appeared in citation of published article and may be found at https://aip.scitation.org/doi/10.1063/1.5093351 . |
| Type | article |
| File Information | 1.5093351.pdf |



[Instructions for use](#)

In situ X-ray photoelectron spectroscopy using a conventional Al-K α source and an environmental cell for liquid samples and solid-liquid interfaces

Cite as: Appl. Phys. Lett. **114**, 173702 (2019); <https://doi.org/10.1063/1.5093351>

Submitted: 20 February 2019 . Accepted: 16 April 2019 . Published Online: 30 April 2019

Raimu Endo, Daisuke Watanabe, Masaru Shimomura, and Takuya Masuda



View Online



Export Citation



CrossMark

ARTICLES YOU MAY BE INTERESTED IN

[Acoustically modulated optical emission of hexagonal boron nitride layers](#)

Applied Physics Letters **114**, 171104 (2019); <https://doi.org/10.1063/1.5093299>

[Large photovoltaic response in rare-earth doped BiFeO₃ polycrystalline thin films near morphotropic phase boundary composition](#)

Applied Physics Letters **114**, 173901 (2019); <https://doi.org/10.1063/1.5090911>

[Strain measurement of a channel between Si/Ge stressors in a tri-gate field effect transistor utilizing moiré fringes in scanning transmission microscope images](#)

Applied Physics Letters **114**, 172103 (2019); <https://doi.org/10.1063/1.5084161>

Lock-in Amplifiers up to 600 MHz

starting at

\$6,210



Zurich Instruments

Watch the Video



AIP
Publishing

In situ X-ray photoelectron spectroscopy using a conventional Al-K α source and an environmental cell for liquid samples and solid-liquid interfaces

Cite as: Appl. Phys. Lett. **114**, 173702 (2019); doi: [10.1063/1.5093351](https://doi.org/10.1063/1.5093351)

Submitted: 20 February 2019 · Accepted: 16 April 2019 ·

Published Online: 30 April 2019



View Online



Export Citation



CrossMark

Raimu Endo,^{1,2,3} Daisuke Watanabe,⁴ Masaru Shimomura,⁴ and Takuya Masuda^{1,2,3,a)}

AFFILIATIONS

¹Graduate School of Chemical Sciences and Engineering, Hokkaido University, Sapporo, Hokkaido 060-0810, Japan

²Global Research Center for Environment and Energy Based Nanomaterials Science (GREEN), National Institute for Materials Science (NIMS), Tsukuba, Ibaraki 305-0044, Japan

³Research Center for Advanced Measurement and Characterization, National Institute for Materials Science (NIMS), Tsukuba, Ibaraki 305-0044, Japan

⁴Graduate School of Integrated Science and Technology, Shizuoka University, 3-5-1 Johoku, Nakaku, Hamamatsu, Shizuoka 432-8561, Japan

^{a)} Author to whom correspondence should be addressed: MASUDA.Takuya@nims.go.jp

ABSTRACT

X-ray photoelectron spectroscopy (XPS), which intrinsically requires vacuum, was used to characterize chemical species in a liquid using laboratory XPS apparatus equipped with a conventional Al-K α source and an environmental cell with an ultra-thin silicon nitride membrane as a quasi-transparent window for the transmission of X-rays and photoelectrons. Aqueous solutions of cesium chloride at different concentrations were encapsulated in the cells, and the membrane in contact with the solution was irradiated with X-rays to collect the photoelectrons emitted from the chemical species in a liquid through the membrane. Cs 4d photoelectron peaks were observed, and the peak intensity increased proportionally with the concentration. Thus, the quantitative analysis of solution species by this method is demonstrated.

Published under license by AIP Publishing. <https://doi.org/10.1063/1.5093351>

X-ray photoelectron spectroscopy (XPS), which is employed to nondestructively analyze the composition, the oxidation states, and the chemical bonding of elements at a solid surface, is one of the indispensable techniques for research and development. In XPS, since photoelectrons emitted by a sample when irradiated with X-rays are detected by an electron analyzer, vacuum conditions are essential to prevent significant loss of intensity due to the scattering of photoelectrons in gas and liquid phases. However, tremendous efforts have been devoted to utilize XPS for analyzing liquid samples¹ and solid-liquid interfaces.²⁻⁴

Siegbahn *et al.* performed pioneering photoelectron spectroscopy of liquid samples using a technique called “liquid jet” in the 1970s,⁵ shortly after the development of XPS by their group. In this system, a flowing liquid column was generated with a liquid nozzle placed in a vacuum chamber, and the photoelectrons emitted from the surface of the liquid column were detected by a differentially pumped electron analyzer under high vacuum ($<2 \times 10^{-5}$ Torr). This technique has been utilized for characterizing a wide variety of systems such as water,⁶ organic solvents,⁷ ionic species,⁸ and nanoparticles in a liquid phase.⁹⁻¹¹

Apart from electrochemical XPS systems equipped with an electrochemical cell and an electron analyzer,¹²⁻¹⁵ a few innovative techniques for analyzing liquid samples and solid-liquid interfaces have been developed. One is the utilization of ionic liquids, the vapor pressure of which is almost zero even in vacuum. Electrochemical processes taking place at the ionic liquid-electrode interfaces have been investigated by detecting photoelectrons emitted from the surfaces of ionic liquids and electrodes.¹⁶⁻¹⁸ Although these studies provide key information, the physicochemical properties of ionic liquids are significantly different from those of water or organic solvents. Therefore, an alternative approach is required for the analysis of such ordinary liquids.

In combination with near ambient pressure (NAP)-XPS, which can be used to analyze solid-liquid or solid-gas interfaces under relatively low vacuum conditions using a differential pumping system,^{2,19-23} a “dip and pull” method has been utilized for a thin liquid-layer-coated electrode surface partially pulled up from a liquid reservoir placed in an analysis chamber.^{24,25} When the liquid layer is very thin (~ 10 nm), not only the solution species but also the species adsorbed onto the electrode surface and the oxidation state of the

electrode surfaces can be analyzed by detecting the photoelectrons emitted from the electrified interfaces through the liquid layer.^{26,27}

Another approach involves the utilization of an environmental cell in which a liquid or gas sample can be sealed using a thin membrane such as graphene oxide,²⁸ Si,²⁹ and graphene^{30–33} as a window for transmitting X-rays/photoelectrons and a separator between vacuum and the environment. In contrast to the dip and pull method, this technique, in principle, does not impose a limitation on the thickness of the liquid phase, because neither X-rays nor photoelectrons pass through the liquid. However, the photoelectron intensity could get substantially attenuated while passing through the membrane because of the scattering of photoelectrons. For example, the attenuation length of photoelectrons is typically approximately several nanometers³⁴ in the case of Mg- $K\alpha$ ($h\nu = 1253.6$ eV) or Al- $K\alpha$ ($h\nu = 1486.7$ eV) excitation, which is widely used in laboratory apparatus. Therefore, utilization of hard X-rays at synchrotron radiation facilities was considered as an effective approach to detect the photoelectrons through the membrane, because it can significantly increase the attenuation length of photoelectrons. However, it brings about an inevitable reduction in the photoionization cross-sections. Therefore, it is desirable to introduce environmental cells into the common laboratory apparatus. The utilization of soft X-rays and thin silicon nitride membranes that have been proposed and demonstrated previously,^{28,35} combined with the recent improvements in the laboratory XPS instrument, enables one to revisit this issue.

In our previous study, an environmental cell equipped with a 15 nm-thick Si membrane as a quasi-transparent window was fabricated.²⁹ Then, an *in situ* XPS study of electrochemical oxidation of Si at the Si-water interface was carried out under bias application by employing hard X-rays (~ 6 keV) from a synchrotron source. In the present study, we constructed an environmental cell with a 5 nm-thick silicon nitride membrane and demonstrate XPS of liquid samples in the cell using laboratory-based apparatus with a conventional Al- $K\alpha$ source. Solutions of cesium chloride in water at various concentrations were encapsulated in the cells, and the photoelectrons emitted from the chemical species in the solution were quantitatively detected by studying the concentration-dependence of the photoelectron intensity.

Solutions of cesium chloride (CsCl; Kanto Kagaku, 98.0%) at different concentrations (0.6, 1.1, 2.6, and 4.5 M) were prepared using pure water from a Milli-Q system (Merck Millipore). Because the silicon nitride membrane is most probably non-stoichiometric in composition, it is denoted SiN.²⁸ SiN microchips (SiMPore, Inc.) were applied as a window of the environmental cell, which can encapsulate a liquid sample in its cavity. The microchip has a 5 nm-thick quasi-transparent SiN membrane with a dimension of $30 \times 30 \mu\text{m}$ at the center of a 3-mm-long Si microchip, as shown in Figs. 1(a)–1(c).

Figure 1(d) illustrates the dimension of the environmental cell and the principle of XPS for analyzing liquid samples. The procedure for preparing the environmental cell has been reported previously.²⁹ Plasma treatment (PIB-10, Vacuum Device) was performed on SiN to obtain a hydrophilic SiN surface, and a droplet of the solution was placed on the surface. After combining the chip with a piece of conductive copper tape (Seiwa Electric MFD), the solution was sealed by applying a sealant available for vacuum (Torr Seal[®], Varian), and then dried at room temperature under ambient conditions. The resulting cells were screened for the XPS measurements by observing them with an optical microscope, as shown in Fig. 1(e).

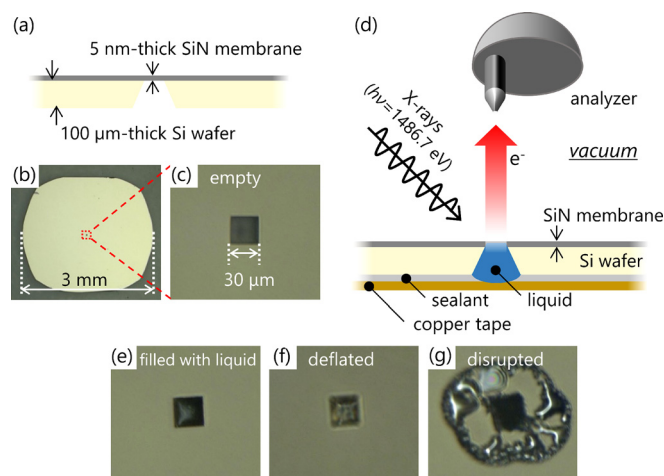


FIG. 1. (a) Cross-sectional and (b) top views of the Si chip and (c) a magnified image of the quasi-transparent SiN membrane. (d) Schematic illustration of the environmental cell and configuration of the XPS system. Photographs of the quasi-transparent windows used for screening: (e) filled with a liquid sample, (f) deflated, and (g) disrupted causing leakage of the liquid sample.

XPS was performed on an AXIS NOVA (Shimadzu Kratos) equipped with a monochromatic Al- $K\alpha$ source at an operating X-ray power of 300 W without neutralizing charge using an electron gun. The photoelectron take-off angle (θ) was fixed at 0° , and the aperture of the hemispherical analyzer was placed perpendicular to the sample surface. The analysis area was a spot with a diameter of $110 \mu\text{m}$, and the energy of the photoelectrons passing through the analyzer (pass energy) was 160 eV. The vacuum pressure in the analysis chamber was $\sim 5 \times 10^{-8}$ Torr.

As a reference sample, CsCl solution was drop-casted on a hydrophilic SiN membrane, and the dried sample was analyzed with and without charge neutralization.

In general, a thinner membrane has better transparency for photoelectrons, although its mechanical strength is weaker (the membrane can be ruptured easily). The attenuation ratio, I_s/I_0 , of photoelectrons for three different membranes with thicknesses of 5, 10, and 15 nm was estimated using the following equation:

$$I_s/I_0 = \exp(-d/\lambda_{\text{IMFP}} \cdot \cos \theta), \quad (1)$$

where d , λ_{IMFP} , and θ are the thickness of the membrane, the inelastic mean free path of electrons calculated using the TPP-2M equation,³⁴ and the take-off angle of photoelectrons (0°), respectively. We assumed a stoichiometric Si_3N_4 membrane for the calculation of λ_{IMFP} . Figure 2 shows the attenuation ratio of the photoelectron through the 5, 10, and 15 nm-thick Si_3N_4 membranes as a function of the kinetic energy of photoelectrons. The results suggest that, in the case of the 5 nm-thick Si_3N_4 membrane, $\sim 20\%$ of photoelectrons ejected from the Cs 4d level upon exciting with Al- $K\alpha$ (Kinetic energy = 1410 eV) pass through the membrane without inelastic scattering, whereas only 4% and 0.8% of the photoelectrons pass through 10 and 15 nm-thick membranes, respectively. Thus, the 5 nm-thick SiN membrane was chosen as a window for the environmental cells.

The red curve in Fig. 3 is the Cs 4d photoelectron spectrum acquired from a cell filled with 4.5 M aqueous CsCl solution. A doublet

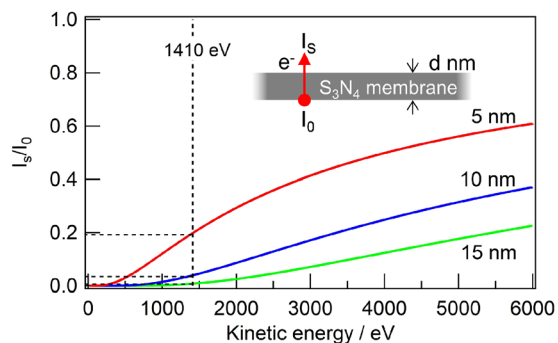


FIG. 2. Attenuation ratio of the photoelectron intensity (I_s/I_0) passing through the 5 nm (red), 10 nm (blue), and 15 nm-thick (green) Si_3N_4 membranes as a function of the kinetic energy of photoelectrons.

peak corresponding to Cs $4d_{5/2}$ and $4d_{3/2}$ is observed at 75.8 and 78.1 eV, respectively. The ratio of the integrated peak area ($4d_{5/2}:4d_{3/2}$) was calculated to be approximately 3:2 by curve fitting, which is in good agreement with the theoretical value for the split d orbital peaks.³⁶ The Cs 4d peaks were obtained only from the quasi-transparent window part, indicating that the observed Cs 4d signals indeed originated from the aqueous CsCl solution encapsulated in the cell and detected through the membrane.

The photoelectrons from dried CsCl powder (reference sample) deposited on the membrane were collected through the membrane without charge neutralization. The Cs 4d peak shifted to a higher binding energy by more than 5 eV (blue curve in Fig. 3) with respect to that of the liquid sample (red curve in Fig. 3). In addition, the ratio of the Cs $4d_{5/2}$ and $4d_{3/2}$ peaks was found to be approximately 1:1, which significantly deviates from the theoretical value of 3:2. This change is attributed to the very low conductivity of the solid CsCl, resulting in charge-up due to the emission of photoelectrons. This difference between the solid and liquid samples suggests that the liquid, water, was certainly sealed in the cell and acted as a conductive medium for electrons. When solid CsCl was subjected to charge neutralization using an electron gun that supplies low-energy electrons to compensate

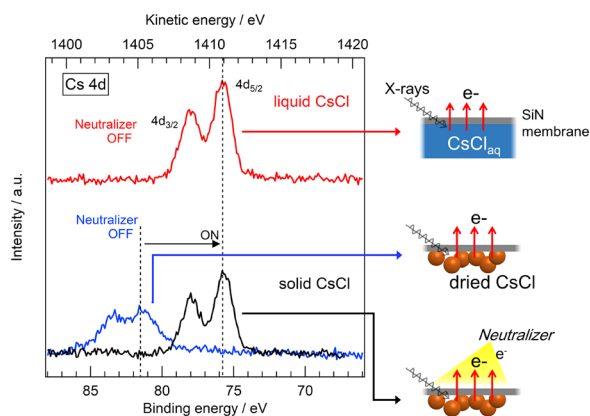


FIG. 3. Cs 4d photoelectron spectra acquired from the cells filled with a 4.5 M aqueous CsCl solution without charge neutralization (red curve) and a dry solid CsCl sample without (blue curve) and with charge neutralization (black curve).

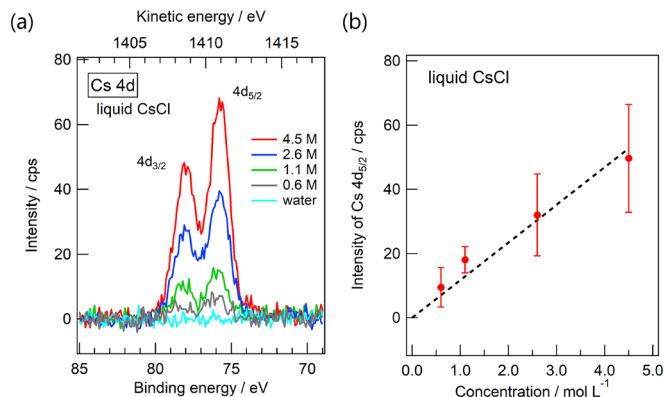


FIG. 4. (a) Cs 4d photoelectron spectra of pure water and 0.6, 1.1, 2.6, and 4.5 M aqueous CsCl solutions in environmental cells. Each spectrum was collected with an acquisition time of ~ 200 min. Linear approximation was adopted for background subtraction. (b) Concentration-dependence of the intensity of the Cs $4d_{5/2}$ peak. The black dashed line is a linear fit to the data.

for the charge due to the ejected photoelectrons, a doublet Cs 4d peak with the theoretical ratio of peak intensity was observed at almost the same energy (black curve in Fig. 3) as that of the aqueous solution (red curve in Fig. 3), confirming that the cesium ions observed as a red curve in Fig. 3 certainly existed in the liquid phase.

The quantitative analysis of cesium ions in solutions was performed as shown in Fig. 4. The intensity of the Cs $4d_{5/2}$ peak increased in proportion to the concentration of the CsCl solution when the cells filled with aqueous CsCl solutions at different concentrations (0.6, 1.1, 2.6, and 4.5 M) and pure water were analyzed. The peak area ratios of Cs 4d/Si 2s and Cs 4d/Si 2p also increased proportionally with the concentration of CsCl, as shown in Fig. S2 (supplementary material). This result clearly indicates the capability of this technique for quantitative characterization of chemical species in a solution. Meanwhile, the position of the Cs $4d_{5/2}$ peak at each concentration remains almost constant (standard deviation ± 0.13 eV), suggesting that the oxidation state of cesium ions was almost identical. Although the Cl 2p and O 1s regions were also analyzed to evaluate the chloride ions and liquid H_2O in the aqueous solution, these peaks were not clearly observed because of the peak overlap with other strong spectral features. The details are summarized in the supplementary material.

In conclusion, we fabricated environmental cells filled with CsCl aqueous solutions of various concentrations using a 5 nm-thick SiN membrane as a transparent window for the transmission of X-rays and photoelectrons, and demonstrated XPS analysis of liquid samples. The Cs 4d photoelectrons passing through the membrane were detected using laboratory XPS apparatus equipped with a conventional Al- $K\alpha$ source. Furthermore, the peak intensity increased proportionally with the concentration of the solutions, proving the capability of quantitative XPS analysis of chemical species in a solution enclosed in the cell, in a laboratory. Application of this technique for investigating electrochemical processes at solid-liquid interfaces is under progress in our laboratory.

See supplementary material for the wide scan and narrow scan spectra.

The present work was partially supported by JSPS KAKENHI Grant Nos. JP16K13941 and JP18H02077 and by MEXT Program for Development of Environmental Technology using Nanotechnology from the Ministry of Education, Culture, Sports, Science and Technology, Japan.

REFERENCES

- ¹B. Winter and M. Faubel, *Chem. Rev.* **106**(4), 1176–1211 (2006); B. Winter, *Nucl. Instrum. Methods Phys. Res., Sect. A* **601**(1–2), 139–150 (2009).
- ²M. Salmeron and R. Schlogl, *Surf. Sci. Rep.* **63**(4), 169–199 (2008).
- ³L. Trotochaud, A. R. Head, O. Karslioglu, L. Kyhl, and H. Bluhm, *J. Phys. Condens. Matter* **29**(5), 053002 (2017).
- ⁴T. Masuda, *Top. Catal.* **61**(20), 2103–2113 (2018).
- ⁵H. Siegbahn and K. Siegbahn, *J. Electron. Spectrosc. Relat. Phenom.* **2**(3), 319–325 (1973); H. Siegbahn, L. Asplund, P. Kelfve, K. Hamrin, L. Karlsson, and K. Siegbahn, *J. Electron. Spectrosc. Relat. Phenom.* **5**(1), 1059–1079 (1974); H. Siegbahn, L. Asplund, P. Kelfve, and K. Siegbahn, *ibid.* **7**(5), 411–419 (1975).
- ⁶B. Winter, R. Weber, W. Widdra, M. Dittmar, M. Faubel, and I. V. Hertel, *J. Phys. Chem. A* **108**(14), 2625–2632 (2004); B. Winter, E. F. Aziz, U. Hergenhanh, M. Faubel, and I. V. Hertel, *J. Chem. Phys.* **126**(12), 124504 (2007).
- ⁷K. A. Perrine, M. H. C. Van Spyk, A. M. Margarella, B. Winter, M. Faubel, H. Bluhm, and J. C. Hemminger, *J. Phys. Chem. C* **118**(50), 29378–29388 (2014).
- ⁸B. Winter, R. Weber, P. M. Schmidt, I. V. Hertel, M. Faubel, L. Vrbka, and P. Jungwirth, *J. Phys. Chem. B* **108**(38), 14558–14564 (2004).
- ⁹J. Söderström, N. Ottosson, W. Pokapanich, G. Öhrwall, and O. Björneholm, *J. Electron. Spectrosc. Relat. Phenom.* **184**(7), 375–378 (2011).
- ¹⁰M. A. Brown, A. Belouqui Redondo, M. Sterrer, B. Winter, G. Pacchioni, Z. Abbas, and J. A. van Bokhoven, *Nano Lett.* **13**(11), 5403–5407 (2013).
- ¹¹G. Olivieri and M. A. Brown, *Top. Catal.* **59**(5–7), 621–627 (2016).
- ¹²T. Mayer, M. Lebedev, R. Hunger, and W. Jaegermann, *Appl. Surf. Sci.* **252**(1), 31–42 (2005).
- ¹³M. V. Lebedev, W. Calvet, B. Kaiser, and W. Jaegermann, *J. Phys. Chem. C* **121**(16), 8889–8901 (2017).
- ¹⁴M. Wakisaka, S. Mitsui, Y. Hirose, K. Kawashima, H. Uchida, and M. Watanabe, *J. Phys. Chem. B* **110**(46), 23489–23496 (2006).
- ¹⁵R. A. Wong, Y. Yokota, M. Wakisaka, J. Inukai, and Y. Kim, *J. Am. Chem. Soc.* **140**(42), 13672–13679 (2018).
- ¹⁶A. W. Taylor, F. Qiu, I. J. Villar-Garcia, and P. Licence, *Chem. Commun.* **0**(39), 5817–5819 (2009).
- ¹⁷R. Wibowo, L. Aldous, R. M. J. Jacobs, N. S. A. Manan, and R. G. Compton, *Chem. Phys. Lett.* **517**(1–3), 103–107 (2011).
- ¹⁸C. Y. Tang, R. T. Haasch, and S. J. Dillon, *Chem. Commun.* **52**(90), 13257–13260 (2016).
- ¹⁹H. S. Casalongue, S. Kaya, V. Viswanathan, D. J. Miller, D. Friebe, H. A. Hansen, J. K. Norskov, A. Nilsson, and H. Ogasawara, *Nat. Commun.* **4**(1), 2817 (2013).
- ²⁰Y. Takagi, H. Wang, Y. Uemura, E. Ikenaga, O. Sekizawa, T. Uruga, H. Ohashi, Y. Senba, H. Yamoto, H. Yamazaki, S. Goto, M. Tada, Y. Iwasawa, and T. Yokoyama, *Appl. Phys. Lett.* **105**(13), 131602 (2014).
- ²¹S. Nemsak, A. Shavorskiy, O. Karslioglu, I. Zegkinoglou, A. Rattanachata, C. S. Conlon, A. Keqi, P. K. Greene, E. C. Burks, F. Salmassi, E. M. Gullikson, S. H. Yang, K. Liu, H. Bluhm, and C. S. Fadley, *Nat. Commun.* **5**, 5441 (2014).
- ²²V. A. Saveleva, V. Papaefthimiou, M. K. Daletou, W. H. Doh, C. Ulhaq-Bouillet, M. Diebold, S. Zafeiratos, and E. R. Savinova, *J. Phys. Chem. C* **120**(29), 15930–15940 (2016).
- ²³V. Streibel, M. Hävecker, Y. Yi, J. J. Velasco-Vélez, K. Skorupska, E. Stotz, A. Knop-Gericke, R. Schlögl, and R. Arrigo, *Top. Catal.* **61**(20), 2064–2084 (2018).
- ²⁴S. Axnanda, E. J. Crumlin, B. Mao, S. Rani, R. Chang, P. G. Karlsson, M. O. Edwards, M. Lundqvist, R. Moberg, P. Ross, Z. Hussain, and Z. Liu, *Sci. Rep.* **5**, 9788 (2015).
- ²⁵M. F. Lichterman, S. Hu, M. H. Richter, E. J. Crumlin, S. Axnanda, M. Favaro, W. Drisdell, Z. Hussain, T. Mayer, B. S. Brunschwig, N. S. Lewis, Z. Liu, and H.-J. Lewerenz, *Energy Environ. Sci.* **8**(8), 2409–2416 (2015).
- ²⁶H. Ali-Löyty, M. W. Louie, M. R. Singh, L. Li, H. G. Sanchez Casalongue, H. Ogasawara, E. J. Crumlin, Z. Liu, A. T. Bell, A. Nilsson, and D. Friebe, *J. Phys. Chem. C* **120**(4), 2247–2253 (2016).
- ²⁷M. Favaro, B. Jeong, P. N. Ross, J. Yano, Z. Hussain, Z. Liu, and E. J. Crumlin, *Nat. Commun.* **7**, 12695 (2016).
- ²⁸A. Kolmakov, D. A. Dikin, L. J. Cote, J. Huang, M. K. Abyaneh, M. Amati, L. Gregoratti, S. Gunther, and M. Kiskinova, *Nat. Nanotechnol.* **6**(10), 651–657 (2011).
- ²⁹T. Masuda, H. Yoshikawa, H. Noguchi, T. Kawasaki, M. Kobata, K. Kobayashi, and K. Uosaki, *Appl. Phys. Lett.* **103**(11), 111605 (2013); T. Masuda and K. Uosaki, *J. Electron. Spectrosc. Relat. Phenom.* **221**, 88–98 (2017).
- ³⁰J. Kraus, R. Reichelt, S. Gunther, L. Gregoratti, M. Amati, M. Kiskinova, A. Yulaev, I. Vlassioug, and A. Kolmakov, *Nanoscale* **6**(23), 14394–14403 (2014); S. Nemsak, E. Strelcov, T. Duchon, H. Guo, J. Hackl, A. Yulaev, I. Vlassioug, D. N. Mueller, C. M. Schneider, and A. Kolmakov, *J. Am. Chem. Soc.* **139**(50), 18138–18141 (2017).
- ³¹J. J. Velasco-Vélez, V. Pfeifer, M. Havecker, R. S. Weatherup, R. Arrigo, C. H. Chuang, E. Stotz, G. Weinberg, M. Salmeron, R. Schlogl, and A. Knop-Gericke, *Angew. Chem. Int. Ed. Engl.* **54**(48), 14554–14558 (2015); J. J. Velasco-Vélez, V. Pfeifer, M. Havecker, R. Wang, A. Centeno, A. Zurutuza, G. Algara-Siller, E. Stotz, K. Skorupska, D. Teschner, P. Kube, P. Braeuninger-Weimer, S. Hofmann, R. Schlogl, and A. Knop-Gericke, *Rev. Sci. Instrum.* **87**(5), 053121 (2016); A. Knop-Gericke, V. Pfeifer, J. J. Velasco-Vélez, T. Jones, R. Arrigo, M. Havecker, and R. Schlogl, *J. Electron. Spectrosc. Relat. Phenom.* **221**, 10–17 (2017).
- ³²R. S. Weatherup, B. Eren, Y. Hao, H. Bluhm, and M. B. Salmeron, *J. Phys. Chem. Lett.* **7**(9), 1622–1627 (2016).
- ³³L. Nguyen, P. P. Tao, H. Liu, M. Al-Hada, M. Amati, H. Sezen, L. Gregoratti, Y. Tang, S. D. House, and F. F. Tao, *Langmuir* **34**(33), 9606–9616 (2018); L. Nguyen, P. P. Tao, H. Liu, M. Al-Hada, M. Amati, H. Sezen, Y. Tang, L. Gregoratti, and F. F. Tao, *Chem. Commun.* **54**(71), 9981–9984 (2018).
- ³⁴S. Tanuma, C. J. Powell, and D. R. Penn, *Surf. Interface Anal.* **35**(3), 268–275 (2003).
- ³⁵C. E. Bryson III, F. J. Grunthner, and P. J. Grunthner, U.S. patent 6,803,570 B1 (12 October 2004).
- ³⁶C. D. Wagner, L. E. Davis, M. V. Zeller, J. A. Taylor, R. H. Raymond, and L. H. Gale, *Surf. Interface Anal.* **3**(5), 211–225 (1981).